

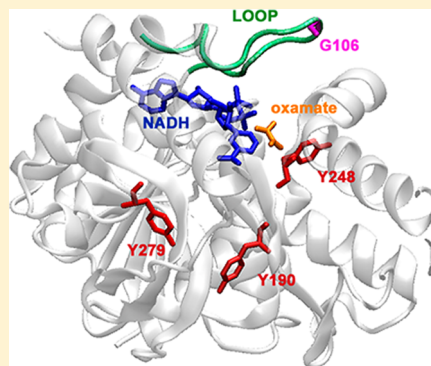
# Large Scale Dynamics of the Michaelis Complex in *Bacillus stearothermophilus* Lactate Dehydrogenase Revealed by a Single-Tryptophan Mutant Study

Beining Nie,<sup>†</sup> Hua Deng,<sup>†</sup> Ruel Desamero,<sup>‡</sup> and Robert Callender<sup>\*,†</sup>

<sup>†</sup>Department of Biochemistry, Albert Einstein College of Medicine, Bronx, New York 10461, United States

<sup>‡</sup>Department of Chemistry, York College, City University of New York, Jamaica, New York 11451, United States

**ABSTRACT:** Large scale dynamics within the Michaelis complex mimic of *Bacillus stearothermophilus* thermophilic lactate dehydrogenase, bsLDH·NADH·oxamate, were studied with site specific resolution by laser-induced temperature jump relaxation spectroscopy with a time resolution of 20 ns. NADH emission and Trp emission from the wild type and a series of single-tryptophan bsLDH mutants, with the tryptophan positions different distances from the active site, were used as reporters of evolving structure in response to the rapid change in temperature. Several distinct dynamical events were observed on the millisecond to microsecond time scale involving motion of atoms spread over the protein, some occurring concomitantly or nearly concomitantly with structural changes at the active site. This suggests that a large portion of the protein–substrate complex moves in a rather concerted fashion to bring about catalysis. The catalytically important surface loop undergoes two distinct movements, both needed for a competent enzyme. Our results also suggest that what is called “loop motion” is not just localized to the loop and active site residues. Rather, it involves the motion of atoms spread over the protein, even some quite distal from the active site. How these results bear on the catalytic mechanism of bsLDH is discussed.



The process of formation of a productive enzymic Michaelis complex is one of narrowing the conformational states of the enzyme–substrate system so that, in its search through all the accessible conformations, the system finds the transition state of the on-enzyme chemical reaction in a timely manner. The process involves numerous dynamical events, such as formation of an encounter complex between the substrate and enzyme with reorientation of the ligand to fit the binding pocket, desolvation, and structural rearrangements in and around the active site to accommodate the ligand and to establish proper contacts necessary for catalysis. These steps include atomic motions and conformational changes on various scales, occurring over a very wide time range, from femtoseconds to milliseconds.<sup>1–4</sup> The details of these changes and motions are essential for understanding the mechanisms of catalysis, but in general, our knowledge of these dynamics within enzyme–substrate systems is very limited. It is clear from earlier studies that enzymes (proteins) exist in an ensemble of conformations, some of which are competent in binding their ligands and others of which bind poorly or not at all (e.g., for LDH<sup>5–7</sup>). It has been shown directly that conformational changes occur within the ensemble of enzyme–substrate Michaelis complexes on various time scales from femtoseconds and picoseconds to milliseconds and slower.<sup>8–10</sup> Here we investigate, using laser-induced temperature-jump spectroscopy, the dynamics of NADH and oxamate binding to thermophilic *Bacillus stearothermophilus* lactate

dehydrogenase (bsLDH) and the dynamics within the bsLDH·NADH·oxamate complex.

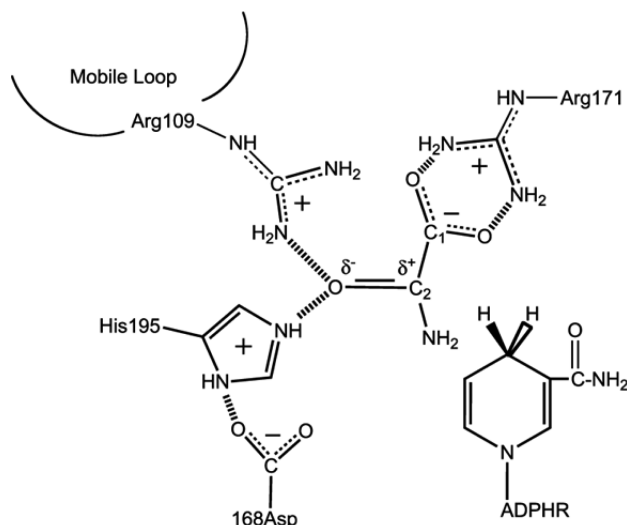
L-Lactate dehydrogenase (LDH, EC 1.1.1.27) catalyzes oxidation of lactate by NAD<sup>+</sup> to produce pyruvate and NADH. In LDH, the substrate binding pocket is sequestered inside the protein ~10 Å from the surface.<sup>11,12</sup> On the basis of several X-ray crystallographic data, oxamate is placed near the nicotinamide ring of the NADH and key protein residues His195, Arg106, and Arg171 (Scheme 1). The C<sub>2</sub>=O bond of oxamate forms hydrogen bonds with His195 and Arg106, while the C<sub>1</sub>OO<sup>−</sup> group forms a salt bridge with Arg171,<sup>13–15</sup> helping to position the substrate. Clarke et al.<sup>16</sup> have also shown that Arg173, which lies on the same helix as Arg171, binds the allosteric effector, fructose 1,6-bisphosphate (FBP). As the substrate approaches the catalytic site, the following events take place: a catalytically key surface loop (residues 98–110) closes over the ligand, bringing residue Arg106 into hydrogen bond contact with the ligand, water leaves the pocket, and the pocket geometry rearranges to allow for favorable interactions between the cofactor and the ligand that facilitate on-enzyme catalysis.<sup>6,17</sup> The bsLDH protein is an interesting variant of the LDH family with a temperature range of activity wider than that of the corresponding mesophiles. It has also been attractive for studies including site-directed mutations that may provide

**Received:** December 28, 2012

**Revised:** February 18, 2013

**Published:** February 21, 2013

# Scheme 1. Active Site Contacts of Pyruvate and NADH Bound to LDH with Key Residues As Determined by X-ray Crystallography<sup>a</sup>



<sup>a</sup>The reaction catalyzed by LDH involves the direct transfer of a hydride ion from C4 of the reduced nicotinamide group of NADH to C2 of pyruvate accompanied by the protonation of pyruvate's keto oxygen, the proton being supplied by His195. It is known that either electrostatic stabilization of the transition state in the pyruvate–lactate interconversion, which contains a highly polarized carbonyl moiety,  $^+C-O^-$ , or destabilization of the  $=C=O$  ground state (or a combination) is responsible for approximately half of the rate enhancement caused by LDH. The other half of the rate enhancement is caused by bringing the cofactor and substrate close together in a proper orientation and “activating” the cofactor for catalysis.

mechanistic information with residue specific structural resolution.<sup>18</sup>

In this study, we investigate the atomic motion within the bsLDH·NADH·oxamate Michaelis complex. To preclude the occurrence of enzyme-catalyzed chemistry that would complicate a kinetic analysis, we used a substrate analogue, oxamate, rather than the natural substrate, pyruvate. Oxamate is isoelectric and isosteric to pyruvate and has been shown to have binding kinetics very similar to that of the actual substrate, pyruvate. We used *T*-jump relaxation profiles to monitor the re-equilibration of a chemical system following an instantaneous increase in temperature induced by a laser pulse tuned to an infrared water band. The re-equilibration results in changes in the concentrations of the species involved, and the transient changes are characterized using spectroscopic probes. The chemical conditions have been arranged so that dynamics within the ternary complex are observed.

First, we probed the fluorescence emission of NADH in wild-type and mutant bsLDH to report on the time evolution of the changes within the NADH environment on the microsecond to millisecond time scale. Second, we determined, on the same time scale, the corresponding tryptophan emissions. Several single-tryptophan bsLDH mutants were constructed to highlight selected positions within bsLDH. These mutants were created by first replacing all tryptophan residues with tyrosine in wild-type bsLDH to create a tryptophan-less template.<sup>19</sup> Earlier studies have shown that neither the tryptophan to tyrosine substitutions nor the subsequent single-tryptophan mutants lead to any substantial changes in the biochemical properties of the enzyme.<sup>20</sup> Into the tryptophan-less template

were introduced further mutations to add a single tryptophan at strategic sites in the protein. We created four single-tryptophan mutants, one (G106W, designations are based on the tryptophan-less mutant, not the wild type) with a tryptophan on the important surface loop<sup>21</sup> and three (Y190W, Y248W, and Y279W) with tryptophan placed varying distances from the active site (Figure 1). In Y248W, the indole ring is

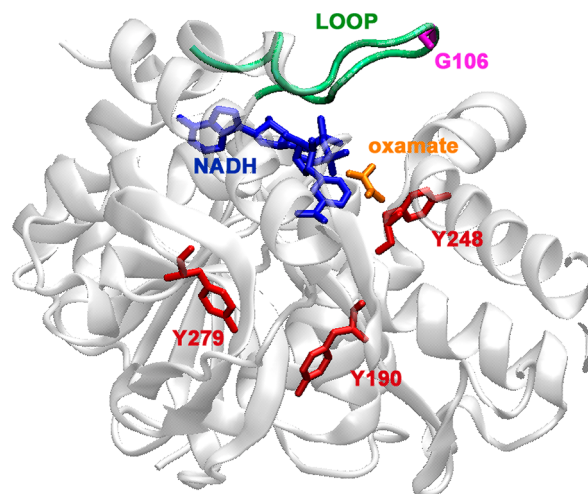


**Figure 1.** Crystal structure of a bsLDH monomer (Protein Data Bank entry 1LDN) depicting the sites of mutation. The sites of tyrosine to tryptophan mutations are colored red. The indole ring of the tryptophan is placed approximately 10.7 Å from the NADH ring for the Y248W mutant, 19.6 Å for Y190W, and 22.3 Å for Y279W. Also highlighted are the cofactor, NADH (blue), oxamate (orange), and the catalytically important loop (green). In a fourth mutant, G106W, the tryptophan is placed on the loop (purple). This figure was generated using VMD.<sup>29</sup>

approximately 10.7 Å from the NADH nicotinamide ring (19.6 Å in Y190W and 22.3 Å in Y279W). Previous time-resolved fluorescence anisotropy studies also suggest that, while the tryptophan in Y248W lies on a very stable helix within the protein, those in Y190W and Y279W do not.<sup>19</sup> The tryptophan in G106W reports mainly on the time evolution of the loop motion, and the tryptophans in Y190W, Y248W, and Y279W report on conformational changes within the protein distant from the binding pocket.

## MATERIALS AND METHODS

**Sample Preparation.** All required reagents were purchased from Sigma-Aldrich Co. (St. Louis, MO) except NADH and oxamate, which were purchased from Roche Diagnostic Corp. (Indianapolis, IN). Reagents were used as received. Samples for *T*-jump measurements were dissolved in 5 mM FBP and 0.1 M triethanolamine (TEA) HCl buffer (pH 6.0) to yield 250 μL of 50–80 μN solutions (concentration of bsLDH subunits). FBP serves as the allosteric activator of the enzyme.<sup>22</sup> Different amounts of NADH and oxamate were added as appropriate to form the binary bsLDH·NADH and ternary bsLDH·NADH·oxamate complexes. Fresh solutions of all reagents were prepared for each experiment.

The bsLDH gene was obtained from genomic DNA from *Geobacillus stearothermophilus* ATCC 12980D, subcloned into the pET3a vector, and transformed into C43(DE3) competent *Escherichia coli* cells. The growth conditions of the transformed

cells and the protein purification were from a published procedure.<sup>14</sup>

The single-tryptophan mutants were prepared following published protocols.<sup>19,21</sup> A tryptophan-less gene, where the three wild-type tryptophan codons (80, 150, and 203) were changed to tyrosine, was cloned to the pET3a vector and transformed into *E. coli* C43(DE3) cells. To obtain the mutants, tryptophan replaced glycine at position 106 (G106W) or tyrosine at position 190 (Y190W), 248 (Y248W), or 279 (Y279W). The growth conditions of the transformed cells and the protein purification procedures were based on a published procedure.<sup>14</sup> The wild-type protein and all four mutants showed catalytic parameters that were the same as published values. The values of the mutants are quite close to that of wild-type bsLDH:  $k_{\text{cat}}$  values of 243, 140, 244, 175, and 182  $\text{s}^{-1}$  for the wild type (WT), G106W, Y190W, Y248W, and Y279W, respectively [taken from the pyruvate side, in 100 mM TEA buffer (pH 6) at 25 °C].<sup>19,21</sup> The  $K_{\text{m}}$  of pyruvate remains at 0.06 mM for all proteins except Y279W, the value of which is 0.04 mM.

**Laser-Induced Temperature Jump.** Laser-induced temperature-jump relaxation spectrometers employed in this study were described previously.<sup>7,10</sup> One of these spectrometers was used for NADH fluorescence kinetic measurements, and another one was used for measurements of tryptophan fluorescence kinetics. In the NADH fluorescence measurements, the excitation light, with a few-milliwatt incident power near 360 nm (351.1 and 363.8 nm lines), was produced with an Innova 70 Ar ion laser (Coherent, Palo Alto, CA). The excitation beam was focused to an  $\sim 0.4$  mm diameter spot in the center of the heated spot of the sample ( $\sim 1.5$  mm diameter). When tryptophan fluorescence detection was used, the fluorescence was excited with an Innova 200 Ar ion laser (Coherent) emitting a group of lines near 300 nm (300.3 and 302.4 nm), with the same  $\sim 0.4$  mm size of the excitation spot on the sample in the center of the  $\sim 1.5$  mm diameter heated spot. NADH fluorescence passes through a 458 nm narrow-band filter with a bandwidth of 40 nm [full width at half-maximum (fwhm)] before reaching the detector, and to select tryptophan emission, a 340 nm narrow-band filter with a 25 nm (fwhm) bandwidth was used (both from Andover, Salem, NH).

## RESULTS AND DISCUSSION

The goal in this study is to concentrate on the dynamics of the conformational ensemble of the bsLDH Michaelis complex. In this work, we employ oxamate as a nonreactive mimic of the substrate pyruvate. Our kinetic studies will then not be influenced by on-enzyme chemistry (i.e., oxidation of NADH). The conditions are at high protein, high NADH, and especially high oxamate concentrations; most studies employed bsLDH, NADH, and oxamate concentrations of 80, 80, and 1200  $\mu\text{M}$ , respectively. This drives the system toward approximately 98% ternary complex, given the  $K_{\text{d}}$  values of NADH with bsLDH and oxamate with the bsLDH·NADH complex. Hence, the  $T$ -jump relaxation kinetic traces should be dominated by unimolecular interconversions within the ternary complex.<sup>23</sup> The fluorescence of NADH is sensitive to its local environment within dehydrogenases and is quite dependent upon local packing interactions.<sup>24</sup> The intrinsic tryptophan fluorescence is also sensitive to the local tryptophan local environment and can be quenched by the nicotinamide ring of bound NADH via Förster resonance energy transfer. The Förster radius for this donor–acceptor pair is  $\sim 15$ – $25$  Å,

depending on the actual values of tryptophan quantum yields.<sup>25</sup> Oxamate binding leads to strong quenching of the fluorescence of bound NADH but does not directly affect tryptophan fluorescence.

**NADH Emission Kinetics.** Figure 2 shows NADH fluorescence 7 °C  $T$ -jump kinetics for wild-type bsLDH to a

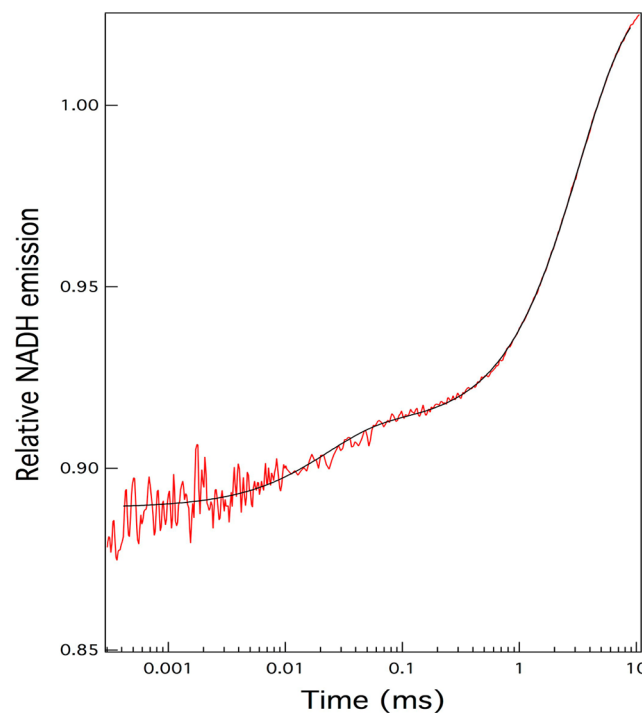


**Figure 2.** NADH fluorescence  $T$ -jump kinetic profile for wild-type bsLDH. The temperature after the  $T$ -jump is 30 °C after a jump of  $\sim 7$  °C. The sample contained 80  $\mu\text{M}$  bsLDH, 80  $\mu\text{M}$  NADH, and 1200  $\mu\text{M}$  oxamate (initial concentrations). The solid line is a three-exponential fit to the data; the results of the fit are given in Table 1.

final temperature of 29.5 °C; the initial concentrations of the various species were 80  $\mu\text{M}$  bsLDH, 80  $\mu\text{M}$  NADH, and 1200  $\mu\text{M}$  oxamate. The relaxation kinetics fit well to a three-exponential function with relaxation rates of 327, 1173, and 45800  $\text{s}^{-1}$ . This kinetic profile is very similar to that found in our studies of the pig heart protein by  $T$ -jump relaxation studies using NADH emission as probe, a strong intensity increase in the time range from submicroseconds to a few milliseconds due to unimolecular transformations between the so-called lightly populated “encounter complex” between LDH·NADH and oxamate, and a substantially populated ternary complex. At 30 °C, the relative NADH quantum yields of emission are 1.0, 1.5, and 0.60 for free NADH, the binary complex, and the ternary complex of bsLDH, respectively, very similar to that of phLDH. In the NADH emission work,<sup>23</sup> an accurate kinetic model (along with microscopic rate constants) could be derived on the basis of extensive studies varying the concentrations of phLDH, NADH, and most importantly oxamate. It was found that the data were fit well by a bimolecular event (the binding of oxamate to the phLDH·NADH complex) and two unimolecular events among three conformations of the phLDH·NADH-oxamate ternary complex. The NADH emission data could be fit equally well to a “sequential” set of events or to a “branched” kinetic scheme whereby the oxamate binds to the binary complex to form a lightly populated encounter



complex, and the more populated ternary complexes interconvert via the encounter complex. The IR  $T$ -jump fit only the branched model.<sup>26</sup> Given the basic similarities between the bsLDH and phLDH enzymes, we expect to obtain a similar kinetic scheme. In fact, IR  $T$ -jump studies of the bsLDH protein yielded results essentially identical to those obtained for the phLDH protein.<sup>27</sup> We construct kinetic models for the data based on our studies and those of other laboratories below, in Conclusions, as a guide for interpreting the data obtained in this study.

Figure 3 shows NADH fluorescence  $T$ -jump kinetics for wild-type bsLDH to a final temperature of 29.5 °C and for the

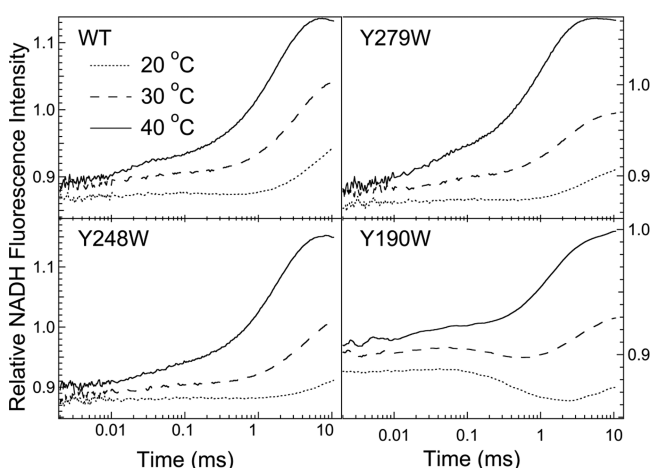


**Figure 3.** NADH fluorescence  $T$ -jump kinetic profiles for wild-type bsLDH and three Trp mutant proteins, Y279W, Y248W, and Y190W. Temperatures after a  $T$ -jump of  $\sim 7$  °C are shown. All samples contained 80  $\mu$ M bsLDH, 80  $\mu$ M NADH, and 1200  $\mu$ M oxamate.

three single-tryptophan mutants, Y279W, Y248W, and Y190W (total concentrations of all components, 80  $\mu$ M bsLDH, 80  $\mu$ M NADH, and 1200  $\mu$ M oxamate). The NADH kinetic profiles for the wild type and Y279W and Y248W mutants are quite similar to each other. At high temperatures, the kinetic traces of NADH within the ternary complex pattern are the same as those for phLDH.<sup>23</sup> Multiexponential fits of the observed kinetic profiles generally yield three time constants within the observational time (see Table 1). The NADH fluorescence  $T$ -jump profiles for the ternary complex of the Y190W mutant differ slightly from the corresponding profiles for wild-type bsLDH and other studied mutants, especially at lower postjump temperatures (Figure 3). The observed exponential rates for the

Y190W bsLDH ternary complex fall within the same time ranges as for other mutants, but the percentage contributions of the components are different.

**Tryptophan Emission Kinetics.** The single-tryptophan mutants afforded us a probe for monitoring local motions within the protein far from the active site. Earlier studies have shown that replacing all the naturally occurring tryptophans with tyrosine in phLDH, or subsequent single-Trp mutants at specific but strategic locations, does not lead to significant changes in the measured biochemical properties of the enzyme.<sup>20</sup> The four single-tryptophan mutants studied here include one with a tryptophan (G106W) on the important surface loop and three (Y248W, Y190W, and Y279W) with a tryptophan placed varying distances from the active site (Figure 1). The  $T$ -jump kinetic profiles of the tryptophan fluorescence within the four mutants are shown in Figure 4.

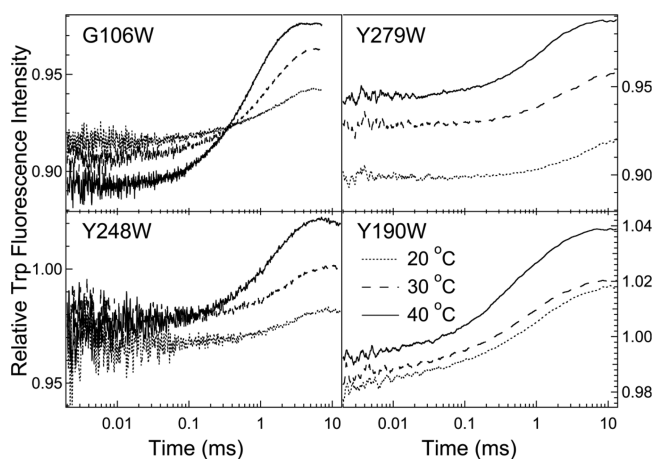


**Figure 4.** Tryptophan fluorescence  $T$ -jump kinetic profiles for the four single-Trp mutant proteins, G106W, Y279W, Y248W, and Y190W. For the G106W mutant, temperatures after an  $\sim 9$  °C  $T$ -jump were 24, 34, and 44 °C, and measurements were taken at pH 7.2. For all other mutants, pH 6.0 buffer was used; temperatures after an  $\sim 7$  °C  $T$ -jump are shown at the bottom right. All samples contained 80  $\mu$ M bsLDH, 80  $\mu$ M NADH, and 1200  $\mu$ M oxamate.

For G106W, wherein the tryptophan is located on the active site loop, the tryptophan fluorescence  $T$ -jump profile at 25 °C fits to a double exponential (Table 1). As the postjump temperature increases, the smaller component of the relaxation kinetics decreases. Because of solubility issues, we were not able to study the G106W mutant as extensively as the other

**Table 1.** Observed Relaxation Rates (Inverse of Relaxation Times) for a 23–30 °C  $T$ -jump for the Ternary Complexes of bsLDH Purified from the Wild Type and the Single-Tryptophan Mutants<sup>a</sup>

	NADH fluorescence $T$ -jump trace			tryptophan fluorescence $T$ -jump trace	
	$1/t_1$ (s <sup>-1</sup> )	$1/t_2$ (s <sup>-1</sup> )	$1/t_3$ (s <sup>-1</sup> )	$1/t_1$ (s <sup>-1</sup> )	$1/t_2$ (s <sup>-1</sup> )
wild type	327 $\pm$ 20; 78%	1173 $\pm$ 500; 8%	45800 $\pm$ 5000; 13%	not measured	not measured
G106W	not measured	not measured	not measured	320 $\pm$ 230; 76%	2300 $\pm$ 1000; 24%
Y190W	303 $\pm$ 11; 56%	3500 $\pm$ 1900; 29%	35500 $\pm$ 2500; 15%	913 $\pm$ 18; 74%	16400 $\pm$ 800; 26%
Y248W	210 $\pm$ 19; 85%	2900 $\pm$ 2400; 5%	26000 $\pm$ 7000; 10%	480 $\pm$ 40	
Y279W	460 $\pm$ 22; 76%	4100 $\pm$ 3500; 7%	19000 $\pm$ 5000; 17%	434 $\pm$ 13	

<sup>a</sup>Most ternary mixtures contain 80  $\mu$ M bsLDH, 80  $\mu$ M NADH, and 1200  $\mu$ M oxamate in TEA buffer at pH 6.0. The only exception was G106W, for which similar mixtures were prepared in TEA buffer at pH 7.2. For G106W, the  $T$ -jump was from 15 to 24 °C. The percent contribution of each component to the amplitude follows each relaxation rate. For comparison,  $T$ -jump IR studies<sup>27</sup> measuring the modulation of the C<sub>2</sub>=O stretch mode of oxamate in the ternary complex of bsLDH yielded two transients at 490 and 1461 s<sup>-1</sup> (at 22 °C).

mutants. G106W bsLDH was previously studied by Holbrook and colleagues,<sup>21</sup> who employed stopped-flow techniques to determine the kinetic profile of Trp emission upon binding of oxamate to the bsLDH-NADH complex and compared this with the results from single-turnover studies of pyruvate to lactate conversion. They found transients for both at 0.125 ms<sup>-1</sup> at 25 °C. This is in good agreement with the current work that shows a transient with a relaxation rate of 0.320 ms<sup>-1</sup> (at the higher final temperature of 30 °C). However, we additionally find a faster transient at 2.3 ms<sup>-1</sup> (presumably simply because of the higher time resolution of this work). Clarke et al.<sup>22</sup> also found two distinct kinetic events in studies of a nitrated pHLDH variant by working at low temperatures to bring both events into the range of conventional mixing studies. Their investigation was to look for loop dynamics, focusing on the issue of loop closure upon substrate binding; the mobile surface loop is found to be open in most crystal structures of LDH-NADH complexes and closed in LDH-NADH-oxamate complexes.<sup>28</sup> Loop motion was assigned to the fast component by Clarke et al. and to the slower component by Holbrook and colleagues.<sup>21</sup> The observed changes in tryptophan emission most likely arise from a modulation of the NADH-Trp radiation-less energy transfer; energy transfer is minimal for the loop-open conformation because the Trp and NADH moieties are very far apart but close for loop-closed structure(s).<sup>22</sup> Taking all the data together, we find it is most plausible that two loop motions take place in the bsLDH-NADH-oxamate complex: one at the relatively slow rate of 0.320 ms<sup>-1</sup> and the other at 2.3 ms<sup>-1</sup> (at 30 °C). Single-turnover studies revealed two rates associated with oxidizing NADH with times similar to those of the tryptophan emission found here.<sup>22</sup> Loop motion, albeit of different structure composition, appears to be part of both these steps.

The tryptophan fluorescence *T*-jump profiles obtained for Y248W (Figure 4), wherein the tryptophan indole ring is located approximately 10.7 Å from the NADH nicotinamide ring on a very stable helix,<sup>19</sup> fit to a single-exponential regardless of the postjump temperature. Interestingly, bsLDH from Y279W exhibits similar single-exponential kinetics despite the fact that the indole ring, located 22.3 Å from the NADH nicotinamide ring, resides on a more flexible helix. Another single-tryptophan bsLDH mutant, Y190W, which has the indole ring located 19.6 Å from the NADH ring on a different flexible helix, exhibited biexponential kinetics (Figure 4 and Table 1).

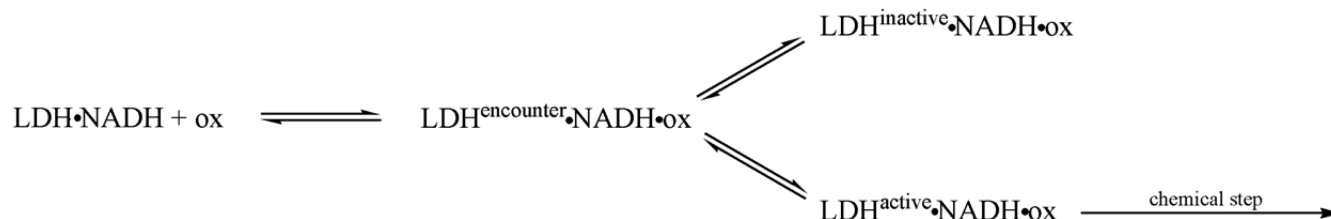
A Förster energy transfer modulation of the Trp emission from the Y190W, Y248W, and Y279W proteins, caused by the release of NADH from the bsLDH-NADH complex, can be a complicating factor in interpreting the Trp emission data because we are interested here in discerning protein motions within the ternary complex. Like the modulation of distance between the Trp-NADH moieties caused by loop motion in the G106W protein, the release of NADH from the binary complex brings about a large change in the Trp-NADH distance. Given the  $K_d$  values of NADH with bsLDH and oxamate with the bsLDH-NADH complex, we estimate the steady state concentrations for the 80/80/1200 WT sample at 28.8 °C are as follows:  $[NADH]_{\text{free}} = 1.4 \mu\text{M}$ ,  $[bsLDH]_{\text{free}} = 1.4 \mu\text{M}$ ,  $[binary] = 0.3 \mu\text{M}$ ,  $[oxamate]_{\text{free}} = 1122 \mu\text{M}$ , and  $[ternary] = 78.3 \mu\text{M}$ . The amount of free bsLDH is 1.0  $\mu\text{M}$  at a temperature 7 °C lower (i.e., before the *T*-jump). If we suppose that all species of the protein bound have basically the same Trp emission quantum yields, then the percentage of the time-

dependent Trp emission signal that is due to NADH release is given by  $[\chi(1.4 \mu\text{M}) + 78.6 \mu\text{M}]/[\chi(1.0 \mu\text{M}) + 79 \mu\text{M}]$ , where  $\chi$  is the relative Trp quantum yield between the free protein and protein bound with NADH. The release of NADH from the binary complex, under these conditions, will take place at ~1 ms. The *T*-jump signals should in Figure 4 change by ~3.0% from a short time (microsecond time scale) to a longer time (millisecond time scale). Although the concentration of the binary complex is very small relative to that of the ternary complex, the Trp emission is very strongly modulated by the release of NADH from the binary complex (i.e., large  $\chi$ ), while the modulation of the Trp emission by local motions within the ternary complex is generally of small amplitude. Using the relationship given above, if  $\chi$  is greater than 8, the reported Trp emission signals in Figure 4 may arise from the release of NADH from the bsLDH-NADH complex. Steady state measurements show that only the Y249W mutant (which has the Trp indole ring closest to bound NADH of the Trp mutants studied) has a large ( $\chi = 10$ ) relative quantum yield; the others are smaller.

## CONCLUSIONS

Several previous studies have revealed a number of features concerning the dynamical nature of LDH and its various complexes. One is that the binary complex exists as an ensemble of substates, some that readily bind substrate and some of the ensemble that do not.<sup>6</sup> The conformation of the binding competent LDH-NADH complex appears to be quite remarkable. The derived structural changes show the active site, normally buried ~10 Å from the protein surface, "pushed up" toward the surface; additionally, there are many changes in hydrogen bonding and hydration throughout the protein.<sup>17</sup> Once the substrate loosely "docks" to the exposed active site (forming what we have called an encounter complex), it is then "dragged" into the heart of the protein to form an ensemble of closely packed conformations apparently with varying degrees of catalytic competence.<sup>9,23,26,27</sup> There is much in all this that resembles the flavor (if not the physics) of a protein-ligand complex in the process of folding. These results suggest substantial collective motions within and across the enzyme, spread over varying time scales, that will be important for the catalytic mechanism.

The interest in this work is to probe these motions in more detail. For this purpose, a set of four single-Trp mutants were constructed for bsLDH based on the work of Holbrook and colleagues.<sup>19</sup> This set of mutant proteins (and others as well) retained basically the same catalytic properties as the wild-type protein but are scattered over diverse locations within the protein (see Figure 1). Hence, it is possible to use the Trp residues as reporters of the surrounding protein dynamics via its modulation of Trp emission. *T*-jump relaxation methods are employed to initiate the kinetic event(s), a method that has a 20 ns resolution in our lab. The tryptophan in G106W reports mainly on the time evolution of the motion of the catalytically important surface loop, while the tryptophans in Y248W, Y190W, and Y279W can report on conformational changes within the proteins distant from the binding pocket (see Scheme 1 and Figure 1). As shown in Results and Discussion, the observed Trp emission transients from the Y279W mutant are due, fully or almost fully, to Förster energy transfer modulated by the release of NADH from the LDH-NADH complex and so are not of interest to us here. We do not discuss the results for this mutant further. The Trp emission

Scheme 2<sup>a</sup>


<sup>a</sup>All results combined<sup>21,22,27</sup> are in agreement and most simply explained by this scheme. The encounter complex presumably has an “open” loop conformation, while the two other conformations of the Michaelis complex, labeled inactive and active, are probably “closed” loop conformations with, however, varying loop structure and atomic arrangements at the active site. The two closed conformations do not appear to directly interconvert, but do so via the encounter complex.

from the Y248W and Y190W mutants contains signatures of local motion of atoms near the Trp reporter.

In stopped-flow emission and absorption studies of pig heart LDH, conducted at  $-16$  to  $8$  °C, so as to slow the kinetics to a time within the stopped-flow resolution, Holbrook and colleagues observed two rates of on-enzyme NADH oxidation, with the slowest corresponding to the steady state  $k_{\text{cat}}$ .<sup>22</sup> The kinetic results were fit to a model that has the protein's Michaelis complex occupy two interconverting conformations with only one able to convert the LDH·NADH·substrate complex to the LDH·NAD<sup>+</sup>·product complex effectively. In Scheme 2, we have graphed the kinetic model of Holbrook et al., modified by our recent kinetic studies.<sup>23,26,27</sup> In our studies, we found that the substrate binds with the LDH·NADH complex to form a “loose” encounter complex. Holbrook et al. had interconversion between the two populated species occurring at the level of the binary complex; the substrate binds or releases between two already preformed binary complex structures. In contrast, in our thinking, the encounter complex collapses to form the two more tightly bound complexes. The tightly bound complexes do not interconvert directly, but rather through the encounter complex.<sup>9,27</sup> This conclusion is based on kinetic–structural studies of bsLDH that probed the key C=O IR stretch band of the bound substrate mimic (oxamate). In that study,<sup>27</sup> three Michaelis (i.e., bsLDH·NADH·oxamate) conformations were found, as indicated by different IR stretching frequencies and the kinetic data, interconverting on times scales with relaxation rates of 490 and 1461 s<sup>−1</sup> (at 22 °C). Only one of the three conformations would be expected to have any propensity for catalysis.<sup>26,27</sup> These Trp emission studies of the G106W protein, taken at near physiological temperatures with an approach that can resolve submillisecond events, are in close agreement [320 and 2300 s<sup>−1</sup> at 30 °C (Table 1)]. Two transients are observed, one near 1 ms, which is the time of the steady state  $k_{\text{cat}}$  for this enzyme.<sup>22</sup> The data from the Y190W mutant report a very similar result (Table 1). Both events appear to involve the motion of the loop given that the Trp reporter in G106W is very sensitive to loop motion, changes in key hydrogen bond patterns at the active site (from the IR studies), and the motion of some parts of the protein far from the active site. These data strongly reinforce the view that the Michaelis complex consists of an ensemble of substates interconverting on time scales faster than catalysis, where some are more competent toward on-enzyme catalysis than others.

Given that the IR studies probe changes in the structure of the active site, specifically the H-bonding patterns between the bound substrate and adjacent active site residues of Arg109 and

His195 (see Scheme 1), and G106W and NADH emission studies probe motion of the surface mobile loop and the structural rigidity of the active site, respectively, we ask if there are motions of residues within the LDH·NADH·oxamate Michaelis complex farther from the active site on similar time scales. The Y248W and Y190W proteins both show a component of protein motion on the 1 ms time scale, very close to the time associated with loop motion and the rate-limiting step to  $k_{\text{cat}}$  (see Table 1), which shows up in the NADH emission profiles as well as the Trp emission. The Y190W protein relaxation spectra show additionally a much faster transient. This result suggests that what is called “loop motion” is not just localized to the loop. Rather, it involves the motion of atoms spread over the protein, even some quite distal from the active site. This is in close accord with our previous molecular dynamics study and experimental work that showed that “closure” of the key surface loop is not a localized hinge motion (as often supposed) but rather a sliding motion happening together with a substantial conformational change in the protein involving many changes to internal hydrogen bonding patterns.<sup>6,17</sup>

## AUTHOR INFORMATION

### Corresponding Author

\*Telephone: (718) 430-3024. Fax: (718) 430-8565. E-mail: robert.callender@einstein.yu.edu.

### Funding

This work was supported by the National Institute of General Medical Sciences of the National Institutes of Health (Grant SP01GM068036).

### Notes

The authors declare no competing financial interest.

## ABBREVIATIONS

LDH, L-lactate dehydrogenase; bsLDH, thermophilic *B. stearothermophilus* lactate dehydrogenase; phLDH, pig heart lactate dehydrogenase; FBP, fructose 1,6-bisphosphate; TEA, triethanolamine; fwhm, full width at half-maximum.

## REFERENCES

- (1) Karplus, M., and McCammon, J. A. (1983) Dynamics of proteins: Elements and function. *Annu. Rev. Biochem.* 53, 263–300.
- (2) Hammes, G. G. (2002) Multiple Conformational Changes in Enzyme Catalysis. *Biochemistry* 41, 8221–8228.
- (3) Frauenfelder, H., Chen, G., Berendzen, J., Fenimore, P. W., Jansson, H., McMahon, B. H., Strope, I. R., Swenson, J., and Young, R. D. (2009) A unified model of protein dynamics. *Proc. Natl. Acad. Sci. U.S.A.* 106, 5129–5134.



- (4) Eisenmesser, E. Z., Bosco, D. A., Akke, M., and Kern, D. (2002) Enzyme dynamics during catalysis. *Science* 295, 1520–1523.
- (5) Gulotta, M., Qiu, L., Rosgen, J., Bolen, D. W., and Callender, R. (2007) Effects of Cell Volume Regulating Osmolytes on Glycerol-3-phosphate Binding to Triphosphate Isomerase. *Biochemistry* 46, 10055–10062.
- (6) Qiu, L., Gulotta, M., and Callender, R. (2007) Lactate Dehydrogenase Undergoes a Substantial Structural Change to Bind its Substrate. *Biophys. J.* 93, 1677–1686.
- (7) Zhadin, N., and Callender, R. (2011) The Effect of Osmolytes on Protein Dynamics in the LDH-Catalyzed Reaction. *Biochemistry* 50, 1582–1589.
- (8) Basner, J. E., and Schwartz, S. D. (2004) Donor-Acceptor Distance and Protein Promoting Vibration Coupling to Hydride Transfer: A possible mechanism for kinetic control in isozymes of human lactate dehydrogenase. *J. Phys. Chem. B* 108, 444–451.
- (9) Deng, H., Brewer, S. H., Vu, D. V., Clinch, K., Callender, R., and Dyer, R. B. (2008) On the Pathway of Forming Enzymatically Productive Ligand-Protein Complexes in Lactate Dehydrogenase. *Biophys. J.* 95, 804–813.
- (10) Zhadin, N., Gulotta, M., and Callender, R. (2008) Probing the Role of Dynamics in Hydride Transfer Catalyzed by Lactate Dehydrogenase. *Biophys. J.* 95, 1974–1984.
- (11) Holbrook, J. J., Liljas, A., Steindel, S. J., and Rossmann, M. G. (1975) Lactate Dehydrogenase. In *The Enzymes*, Vol. XI, pp 191–293, Academic Press, New York.
- (12) Griffith, J. P., and Rossmann, M. G. (1987) M4 Lactate Dehydrogenase Ternary Complex with NAD and Oxamate, Brookhaven Protein Data Bank entry 1LDM.
- (13) Luyten, M. A., Gold, M., Friesen, J. D., and Bryan Jones, J. (1989) On the effects of replacing the carboxylate-binding arginine-171 by hydrophobic tyrosine or tryptophan residues in the L-lactate dehydrogenase. *Biochemistry* 28, 6605–6610.
- (14) Deng, H., Zheng, J., Clarke, A., Holbrook, J. J., Callender, R., and Burgner, J. W. (1994) Source of Catalysis in the Lactate Dehydrogenase System: Ground State Interactions in the Enzyme-Substrate Complex. *Biochemistry* 33, 2297–2305.
- (15) Hart, K. W., Clarke, A. R., Wigley, D. B., Waldman, A. D. B., Chia, W. N., Barstow, D. A., Atkinson, T., Jones, J. B., and Holbrook, J. J. (1987) A strong carboxylate-arginine interaction is important in substrate orientation and recognition in lactate dehydrogenase. *Biochim. Biophys. Acta* 914, 294–298.
- (16) Clarke, A. R., Wigley, D. B., Barstow, D. A., Chia, W. N., Atkinson, T., and Holbrook, J. J. (1987) A single amino acid substitution deregulates a bacterial lactate dehydrogenase and stabilizes its tetrameric structure. *Biochim. Biophys. Acta* 913, 72–80.
- (17) Pineda, J. R. E. T., Callender, R., and Schwartz, S. D. (2007) Ligand Binding and Protein Dynamics in Lactate Dehydrogenase. *Biophys. J.* 93, 1474–1483.
- (18) Atkinson, T., Barstow, D., Chia, W., Clarke, A., Hart, K., Waldman, A., Wigley, D., Wilks, H., and Holbrook, J. J. (1987) Mapping Motion in Large Proteins by Single Tryptophan Probes Inserted by Site-Directed Mutagenesis: Lactate Dehydrogenase. *Biochem. Soc. Trans.* 15, 991–993.
- (19) Smith, C. J., Clarke, A. R., Chia, W. N., Irons, L., Atkinson, T., and Holbrook, J. J. (1991) Detection and Characterization of Intermediates in the Folding of Large Proteins by the Use of Genetically Inserted Tryptophan Probes. *Biochemistry* 30, 1028–1036.
- (20) Roper, D. I., Moreton, K. M., Wigley, D. B., and Holbrook, J. J. (1992) The structural consequences of exchanging tryptophan and tyrosine residues in *B. stearothermophilus* lactate dehydrogenase. *Protein Eng.* 5, 611–615.
- (21) Waldman, A. D., Hart, K. W., Clarke, A. R., Wigley, D. B., Barstow, D. A., Atkinson, T., Chia, W. N., and Holbrook, J. J. (1988) The Use of a Genetically Engineered Tryptophan to Identify the Movement of a Domain of *B. stearothermophilus* Lactate Dehydrogenase with the Process which Limits the Steady-State Turnover of the Enzyme. *Biochem. Biophys. Res. Commun.* 150, 752–759.
- (22) Clarke, A. R., Waldman, A. D. B., Hart, K. W., and Holbrook, J. J. (1985) The Rates of Defined Changes in Protein Structure During the Catalytic Cycle of Lactate Dehydrogenase. *Biochim. Biophys. Acta* 829, 397–407.
- (23) McClendon, S., Zhadin, N., and Callender, R. (2005) The Approach to the Michaelis Complex in Lactate Dehydrogenase: The substrate binding pathway. *Biophys. J.* 89, 2024–2032.
- (24) Velick, S. F. (1958) Fluorescence Spectra and Polarization of Glyceraldehyde-3-phosphate and Lactic Dehydrogenase Coenzyme Complexes. *J. Biol. Chem.* 233, 1455–1467.
- (25) Steinberg, I. Z. (1971) Long-range nonradiative transfer of electronic excitation energy in proteins and polypeptides. *Annu. Rev. Biochem.* 40, 83–114.
- (26) McClendon, S., Vu, D., Clinch, K., Callender, R., and Dyer, R. B. (2005) Structural Transformations in the Dynamics of Michaelis Complex Formation in Lactate Dehydrogenase. *Biophys. J.* 89, L07–L09.
- (27) Deng, H., Vu, D. V., Clinch, K., Desamero, R., Dyer, R. B., and Callender, R. (2011) Conformational heterogeneity within the Michaelis complex of lactate dehydrogenase. *J. Phys. Chem. B* 115, 7670–7678.
- (28) Wigley, D. B., Muirhead, H., Gamblin, S. J., and Holbrook, J. J. (1988) Crystallization of a Ternary Complex of Lactate Dehydrogenase from *Bacillus stearothermophilus*. *J. Mol. Biol.* 204, 1041–1043.
- (29) Humphrey, W., Dalke, A., and Schulten, K. (1996) VMD: Visual molecular dynamics. *J. Mol. Graphics* 14, 33–38.